Research Paper

Attenuation of Humming-Type Noise and Vibration in Vehicle HVAC System Using a Tuneable Dynamic Vibration Absorber

Muhammad Safwan Abdul AZIZ[(1)], Ahmad Zhafran Ahmad MAZLAN[(1)*],
Mohd Hafiz Abdul SATAR[(1)], Muhammad Abdul Rahman PAIMAN[(2)],
Mohd Zukhairi Abd GHAPAR[(2)]

[(1)] *TheVibrationLab, School of Mechanical Engineering, Universiti Sains Malaysia, Engineering Campus*
Penang, Malaysia

[(2)] *Testing and Development, Vehicle Development and Engineering, Proton Holdings Berhad*
Shah Alam, Selangor, Malaysia

*Corresponding Author e-mail: zhafran@usm.my

Heating, ventilation, air conditioning (HVAC) is one of crucial system in a vehicle. Unfortunately, its performance can be affected by the vibration of HVAC components, which subsequently produced unwanted noises. This paper presents an innovative design solution which called as tuneable dynamic vibration absorber (TDVA) to reduce the humming-type noise and vibration in the HVAC system. A detail investigation is carried by developing a lab-scale HVAC model that has the capability to imitate the real HVAC operation in a vehicle. An alternated air-condition (AC) with a fixed blower speed is implied in the study. The analysis of humming-type noise and vibration induced from the HVAC components are performed, and the TDVA is designed and tuned according to the natural frequency of the AC pipe before the attachment. The humming-type noise and vibration characteristics of the HVAC components are compared before and after the implementation of the TDVA. The findings shown that the HVAC model data compares well with the vehicle data, whereby the implementation of TDVA is found to reduce the vibration of the AC pipe by 79% and 61% in both idle and operating conditions and this subsequently improved the humming-type noise of the HVAC system. It also been observed that the TDVA has an effective frequency range around 75–255 Hz and 100–500 Hz for the HVAC model and vehicle systems, respectively.

Keywords: HVAC; humming noise; vibration attenuation; AC pipe; TDVA.

1. Introduction

Facing with increased demands of vehicles, a wide range of aspects need to be covered by industries and researchers to meet the customer requirements. Aside from vehicle features and performance, comfortability is a main key for the customer when purchasing a vehicle. One of the factors that effecting the comfortability and the HVAC system is a major contribution as reported in previous studies (XI *et al.*, 2015). The working principle of this system relies on the circulation of the refrigerant and water to provide a comfortable feel-

ing for the driver and passenger through the convection and conduction in the heating or cooling of surrounding air (SIMION *et al.*, 2016; WANG *et al.*, 2005). Even though comfortability is a subjective term, a lot of concerns have been raised since it is affecting the driving and distracting the focus of the driver. A vehicle with good comfortability will attract more customers and the manufacturers will receive competitive advantages in the market (SINGH *et al.*, 2014).

Vibration and noise are the interrelated elements, which after exceeding certain level, it will lead to uncomfortable feeling. In HVAC system, the total noise

can be contributed by the individual components with specific characteristics (EILEMANN, 1999). The noise generated is airborne, that transmitted through the air (MAVURI *et al.*, 2008). Unfortunately, the study involving HVAC noise characterization is still limitedly available. For example, the study done by THAWANI *et al.* (2013) found that the hissing noise occurred in the operating frequency of 2–10 kHz. The work later expanded by SATAR *et al.* (2021a), on the different operating conditions namely as idle and operating conditions. The authors found that the hissing noise is produced at more specific operating frequency of 4500–5000 Hz for both conditions. Both studies reported that an evaporator is a major HVAC component for the noise generation, due to sudden flow of gas and fluid refrigerant (i.e. R134a) at high pressure and velocity through a narrow passage. SATAR *et al.* (2019) proposed that the clicking and air-rush noises are produced at the operating frequency of 200–300 Hz and 1400–1700 Hz, respectively. They explained that the clicking noise is contributed by the compressor due to the clutch engagement. It is the later effect of R134a circulating during the clutch engagement. Contrarily, the air-rush is contributed by the turbulence effect of airflow in the HVAC blower. Depends on setting of the HVAC system, but it usually happened when the air flows with high velocity through the ducting and ventilation outlets. The turning location near the outlets can caused an irregular flow (WANG, 2010; IMAHIGASHI *et al.*, 2016). In a narrower operating frequency, SATAR *et al.* (2021b) found that the humming noise occurred at the operating frequency of 300–350 Hz and 150–250 Hz for the idle and operating frequency, respectively. The suspected HVAC component contributors are the AC pipe and compressor. In the study, the vibration recorded is dominantly from the compressor, but it partly transferred to the AC pipe in the sequential transmission.

Passive control approaches are the preferable option when dealing with vibration and noise attenuation due to low cost of implementation. This approach involves the reactive or resistive devices that either load the transmission path of the disturbing vibration or absorb the vibrational energy. A review from the literature indicates that ample research is available on the biodegradable natural and synthetic materials. The biodegradable materials such as natural fibre (PARIKH *et al.*, 2006) and jute (FATIMA, MOHANTY, 2011) and the synthetic materials such as micro-perforates (ALLAM, ÅBOM, 2014) and polypropylene (ARENAS, CROCKER, 2010) have been well implemented in the vehicle, which able to reduce noise up to 6–10 dB. Evaluation has been done by SINGH and MOHANTY (2018) that used jute felt and waste cotton to reduce the noise in the HVAC system. The authors also compared the sound absorption coefficients among the natural materials and found that these two have the higher coeffi-

cient. The implementation has been carried out at the major noise source (i.e. recirculation inlet) and able to reduce the sound pressure level (SPL) and loudness level up to 4 dBA and 7 sones, respectively. KURNIAWAN and ROGERS (2011) designed a "V-shape" rubber seal to counter and significant improvement has been achieved by reducing the air flows between the gaps.

Structure dynamic modification (SDM) by using dynamic vibration absorber (DVA) is one of the feasible techniques under the passive approach to channel the vibration energy to a secondary system by adding a secondary mass-spring to the primary system. It has vastly implemented across diverse structures but, least reported in the HVAC system. It works by shifting the natural frequencies, improving the dynamic stabilities, performing the modal synthesis, and optimizing the weights and cost of the structure (HASHI *et al.*, 2016; BRENNAN, 2010; JALILI, ESMAILZADEH, 1998). For example, AHMAD MAZLAN and MOHD RIPIN (2015) applied the SDM method to overcome the limitation of piezoelectric stack actuator in the active suspended handle. By increasing the lower beam stiffness of the handle that supports the actuator, it results in shifting of the modes of the structure beyond the operating frequency range. The implementation able to reduce the vibration transmissibility up to 96%. Another study by WALLACK *et al.* (1989) shows that by adding the rib stiffener and performing the mass modification does change the natural frequencies of the structure. In the study, the comparison has been made using finite element analysis (FEA) and experimental modal analysis (EMA), where the SDM by experiment has fast analysing speed compared to the FEA. A review from the literature indicates that this technique has a concise and economy of mathematical operations (FORMENT, WELARATNA, 1981).

In more practical of DVA application, it has been implemented to the electric grass trimmer, whereby the DVA natural frequency is tuned to be around 220 Hz, to match the operating frequency of the grass trimmer in attenuating the handle vibration (HAO *et al.*, 2011). The results show the average vibration reduction of 82%. Meanwhile, SAIFUDDIN *et al.* (2018) tested the scheme on the motorcycle handle, where the vibration originating from the engine with different road surface roughness at moving speed of 30–50 km/h. It has resulted in vibration attenuation level ranging from 59–68% at a different motorcycle speed. Study from SATAR *et al.* (2019) shows that the application of the DVA can reduced the HVAC component vibration significantly with an effective frequency range of 100–500 Hz. Admittedly, this paper can be regarded as a continuous work from SATAR *et al.* (2019) with more detail humming-type noise and vibration characteristics of the HVAC system and its attenuation using a tuneable dynamic vibration absorber (TDVA). In (SATAR *et al.*, 2019), the study has successfully reduced the vi-

bration of the HVAC system using the DVA scheme, but it is limited to a lab-scale model, which does not prove the reliability of the result obtained for the real vehicle system.

The present paper therein is devoted to study the performance of TDVA scheme on the lab-scale HVAC model, which offers detail humming-type noise and vibration characterization with the verification in real vehicle HVAC system. The primary motivation of this paper is to prove the performance of TDVA in reducing the humming-type noise and vibration of the HVAC system as it is a low cost and using passive control method.

2. Methodology

In this study, the experiment has been conducted in both model and vehicle HVAC systems. The model system is a lab-scale model of the HVAC system, where the investigation in detail can be carried out. The lab-scale model shown in Fig. 1 is built comprising of all HVAC components and have been arranged accordingly as in real vehicle setup. The reliability of the results is then validated with the vehicle system.
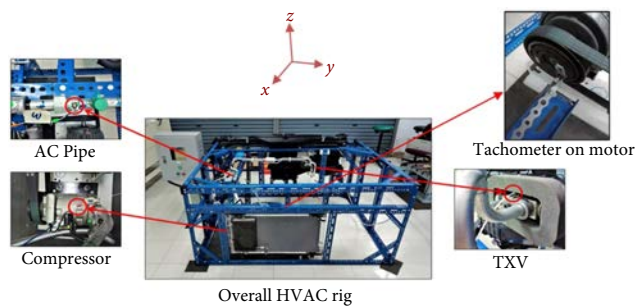

Fig. 1. Overall HVAC model development with sensor's placement.

2.1. Sensor's placement

In both HVAC systems, three different sensors are used for the measurement namely as tachometer, accelerometer, and microphone. The tachometer (Monarch type SPSR-115/300) is used to ensure the engine speed can maintain and operate at desired conditions. Figures 1 and 2 show the attachment of all the sensors in the HVAC model and vehicle systems, respectively. In HVAC model, the tachometer is placed closed with a motor, which used to provide drive action of the compressor. When the engine is operated, the vibration produced by the HVAC components are measured using accelerometer (Kistler type 877A50). The accelerometers are mounted at four locations, which is compressor, thermal expansion valve (TXV) and AC pipe, as shown in Fig. 1. These HVAC components are the suspected contributor to the generation of humming-type noise and vibration.
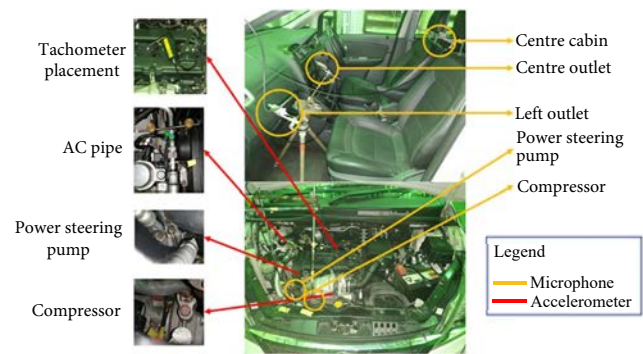

Fig. 2. Sensor's placement in HVAC vehicle.

To validate the presence of noise and vibration of the HVAC model, the measurement is carried out in real vehicle inside a certified anechoic chamber room, as shown in Fig. 2. The similar sensors are used and mounted at the respected locations as in HVAC model. For HVAC vehicle system, the microphone sensor (BSWA type MA231) is mounted at three locations, which is centre cabin (0.7 m from the noise source), centre outlet (0.1 m from the noise source) and left outlet (0.1 m from the noise source) to investigate the noise presence in the vehicle interior space, as shown in Fig. 2. The microphone mounting location is similar to the work done previously by SATAR *et al.* (2021a). All the data measured from both model and vehicle HVAC systems are analysed and compared.

2.2. Experimental modal analysis (EMA)

The inherent dynamic characteristics of HVAC components such as the natural frequency and frequency response function (FRF) can be determined by EMA. FRF is one of the important functions in structural vibration characterization, which establish the input-output measurement relationship as a frequency function (HE, FU, 2001; HAO *et al.*, 2011). In EMA, the work is divided into two steps, which is structure modelling and impact testing. As shown in Fig. 3, a total of 5 and 30 nodes are required to model the AC pipe and compressor in LMS TestLab software.

For the impact testing, an impact hammer (Kistler type 9724A500) is used to hit the test structure to provide an excitation input force. The output response is measured by an accelerometer (Kistler type 9272), which is placed at one of the nodes in Fig. 3. These two instruments are worked based on the roving hammer method, where the accelerometer is fixed at one node and the impact hammer is roved from one node to another. A free-free test condition is implied for this testing to provide more accurate data without the influence of other neighbourhood structures in the HVAC system. The excitation and output response signals are recorded using LMS SCADAS and LMS TestLab software, to obtain the vibration characteristics of each measurement point.
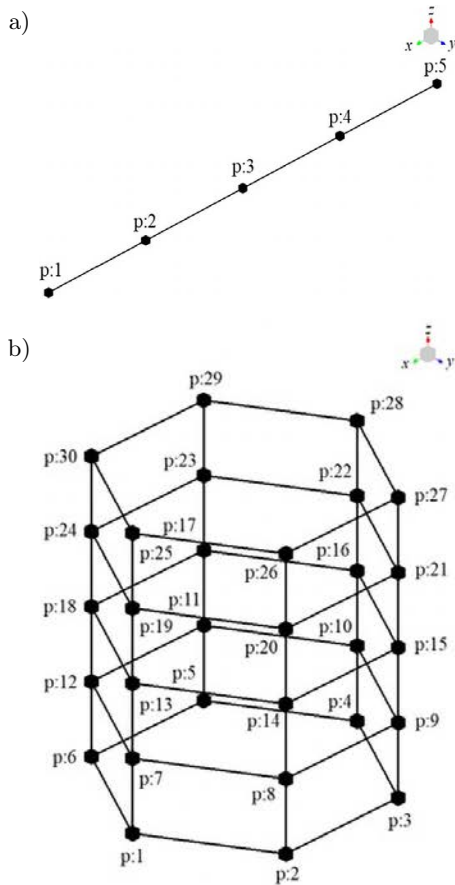
Fig. 3. Geometry model of AC pipe (a) and compressor (b).

2.3. Noise and vibration measurement conditions

Table 1 shows the noise and vibration measurement conditions that been implied for both model and

vehicle HVAC systems. For both systems, the experiment is performed in two different conditions, namely as idle and operating. The idle condition is when the engine speed is maintained at 850 r/min, while for the operating condition, the engine is running from 850–1400 r/min. The engine speed of both model and vehicle are controlled by a speed controller and foot pedal, respectively. To provide reliability results, the measurement of vehicle is conducted in a semi-acoustic chamber to eliminate the environmental noises. All the data is recorded is recorded and analysed using LMS TestLab Signature Throughput Processing and LMS TestLab Sound Diagnosis. As suggested by SINGH *et al.* (2018), the noise measurement is effective around 500 Hz and in the audible range (GREN *et al.*, 2012), hence the study is conducted in a frequency range of 0–600 Hz. All the instruments are calibrated before the measurement to ensure the accuracy of the results obtained.

2.4. Design and implementation of TDVA

Based on study by SATAR *et al.* (2021b), the humming-type noise and vibration can be identified from three major HVAC components, which is compressor, power steering pump and AC pipe. Of these components, the AC pipe is identified as the most suitable component for the application of TDVA based on its location in the engine bay without the necessary modification of AC pipe structure, as this will impact the overall cost of the manufacturer.

The TDVA can be modelled as a second mass-spring system added to the primary system (i.e. AC pipe), as shown in Fig. 4a. From the figure, m and k are the mass and stiffness of the AC pipe while m_a

Table 1. Measurement conditions in the model and vehicle HVAC systems.

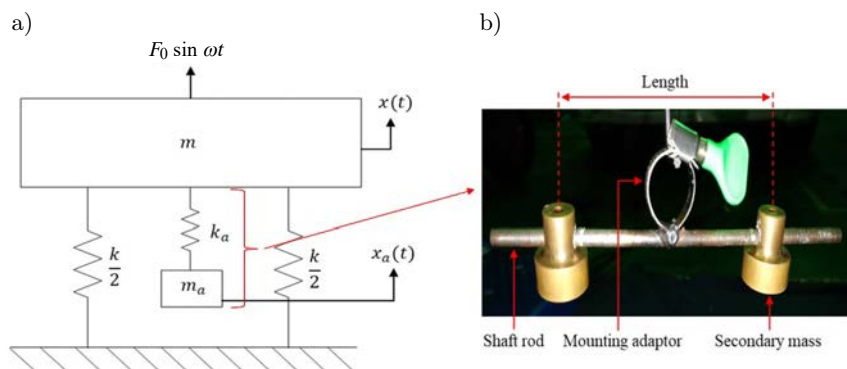| HVAC system	Test conditions	Engine speed [r/min]	AC status	Test locations
Model	Idle	850	On and off	Compressor, AC pipe
	Operating	850–1400		
Vehicle	Idle	850		Engine bay and cabin
	Operating	850–1400		

Fig. 4. TDVA theoretical model (a) and fabricated (b).

and k_a are the mass and stiffness of the TDVA, respectively. The equation of motion for the AC pipe with the TDVA can be written as follows:

$$m\ddot{x} + x(k + k_a) - k_a x_a = F_0 \sin \omega t, \qquad (1)$$

$$m_a \ddot{x}_a + k_a x_a - k_a x = 0. \qquad (2)$$

By dividing Eqs (1) and (2) with m and m_a, respectively, hence:

$$\ddot{x} + \frac{x(k + k_a)}{m} - \frac{k_a x_a}{m} = \frac{F_0}{m} \sin \omega t, \qquad (3)$$

$$\ddot{x}_a + \frac{k_a x_a}{m_a} - \frac{k_a x}{m_a} = 0. \qquad (4)$$

Let's the $\frac{F}{m} \sin \omega t = \frac{F}{m} e^{j\omega t}$ and by assuming the solution in form of:

$$X = x e^{j\omega t}, \qquad (5)$$

$$X_a = x_a e^{j\omega t}. \qquad (6)$$

By substituting Eqs (5) and (6) into (3) and (4), hence:

$$X = \frac{\frac{F}{m}\left(\frac{k_a}{m_a} - \omega^2\right)}{\left(\frac{k+k_a}{m} - \omega^2\right)\left(\frac{k_a}{m_a} - \omega^2\right) - \frac{k_a^2}{m \cdot m_a}}, \qquad (7)$$

$$X_a = \frac{\frac{k_a}{m_a}}{\left(\frac{k_a}{m_a} - \omega^2\right)} X. \qquad (8)$$

From Eq. (7), the vibration displacement of AC pipe will become, $X = 0$ when $\frac{k_a}{m_a} = \omega^2$, where ω is the natural frequency of the secondary mass (TDVA). Therefore, by tuning the natural frequency of TDVA to be the same as excitation frequency, the internal energy of AC pipe can be transferred to the TDVA. Hence the vibration of AC pipe at its operating frequency can be reduced.

In this study, the TDVA is consisted of steel shaft rod k_a and two brass masses of $m_{a1} + m_{a2} = m_a$, that placed on both sides of the rod, as shown in Fig. 4b. The structure is attached to the AC pipe using a mounting adaptor, which is welded to the steel rod. By adjusting the length L between the masses, the DVA can be tuned according to the targeted frequency of the structure using the following equation:

$$L^3 = \frac{3EI}{(2\pi f)^2 \cdot m_a}, \qquad (9)$$

where E is the modulus elastic of the rod, I is the moment of inertia and f is the operating frequency. The L value obtained is adjusted accordingly at the TDVA before the attachment at the AC pipe, as shown in Fig. 5. From the figure, point 2 is selected as it provides sufficient space for the TDVA attachment in the engine bay. From this, the EMA is repeated to observe the effect of TDVA to the natural frequency of the AC pipe.
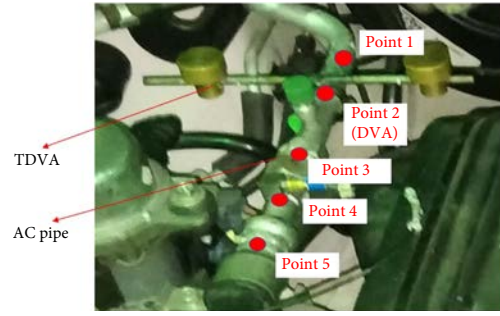

Fig. 5. TDVA attachment points on AC pipe.

3. Results and discussion

3.1. EMA results

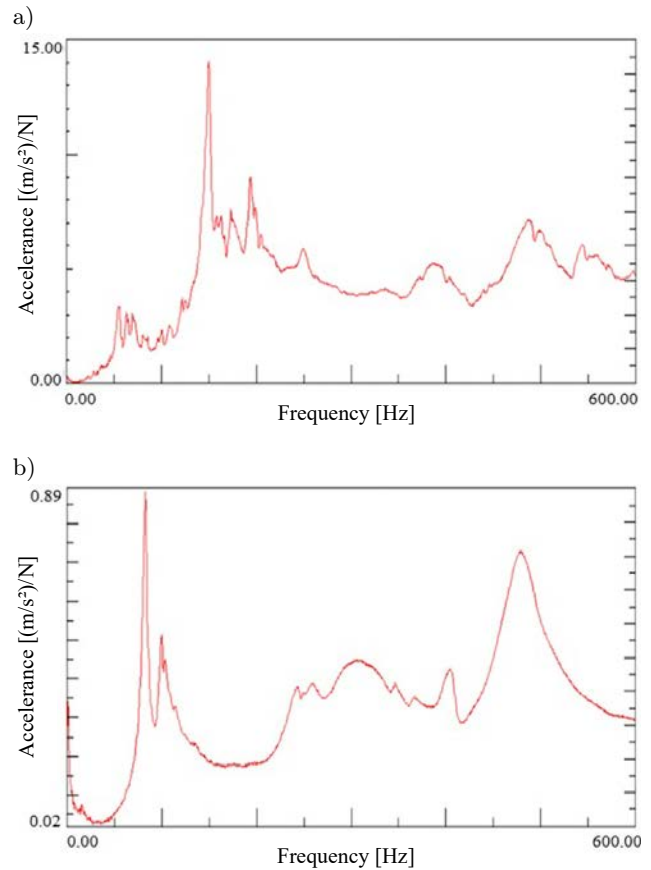Figure 6 shows the FRF of the AC pipe and compressor, respectively.

Fig. 6. FRF of AC pipe (a) and compressor (b).

From the figures, it can be observed that both AC pipe and compressor have the significant peaks of natural frequencies between 50–250 Hz, whereby the highest peak occurred at 148 Hz and 85 Hz for AC pipe and compressor, respectively. This frequency range is corresponded to the region of humming noise and vibration determined by (Satar et al., 2019; 2021b). This subsequently will create a resonance to the AC pipe and

neighbouring HVAC components while increasing the engine speed during the operation condition. A TDVA is proposed in this study to shift the natural frequencies of the AC pipe to be out of region of humming-type noise and vibration.

3.2. Humming noise and vibration

a) Idle condition

Figures 7 shows the fast Fourier transform (FFT) of the acceleration amplitude for the AC pipe and compressor in the HVAC model system, respectively.
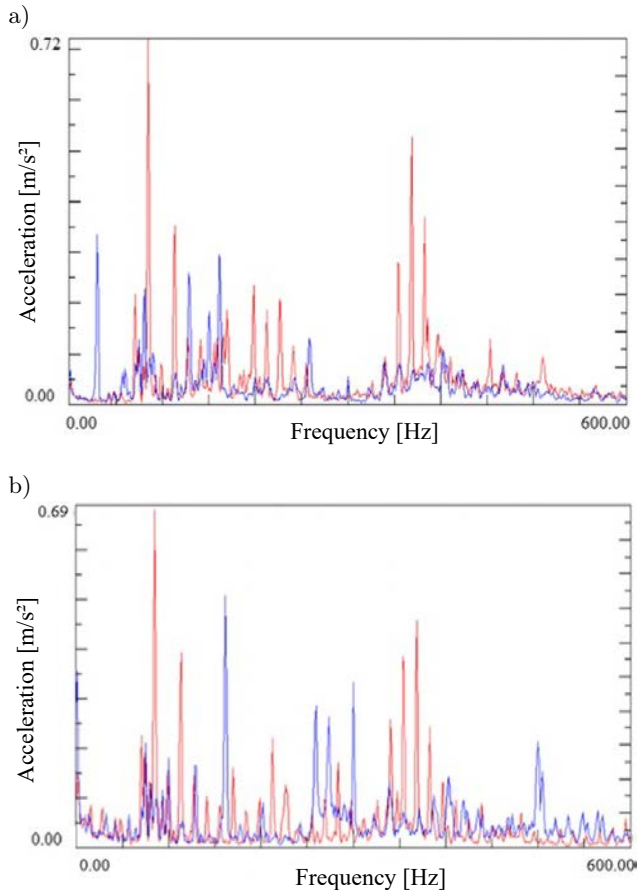
a)

b)

Fig. 7. Acceleration FFT of AC pipe (a) and compressor (b) in the HVAC model; red – AC off, blue – AC on (idle).

From the figures, it can be observed that initially when the AC is off, the acceleration amplitude of AC pipe is high at the frequency below 100 Hz with the amplitude of 0.72 m/s^2. Inversely after the activation of the AC, the amplitude is only reached around 0.20 m/s^2. However, there is a slight increment in amplitude after 100 Hz, due to the effect of AC pipe structural natural frequencies, as shown in Fig. 6a, previously. The higher acceleration amplitude trend when AC is off can be explained by the effect of the vibration that been transferred from the motor in HVAC model system. A similar trend of vibration response can be observed for the compressor in Fig. 7b, as

it has also been affected by the natural frequencies of the compressor structure. This subsequently created the humming-type noise and vibration in the frequency range of 50–250 Hz.

A verification is conducted with the HVAC vehicle system and presented in Fig. 8. As for the AC pipe, the vehicle system has produced a lower acceleration response compared to the model system due to the more stiffer mounting condition in the vehicle engine bay with no disturbances from the motor vibration. However, a similar trend can still be observed for both systems, wherein the acceleration peaks are dominant at humming frequency ranges (50–250 Hz). The trend of different AC effect is occurred due to the compressor engagement processes. When the compressor is engaged, the HVAC is running smoothly and reduces the overall system vibration. This also supported by the flow of refrigerant fluids which results in an increment of the mass and stiffness of the affected HVAC components (SATAR et al., 2021b).
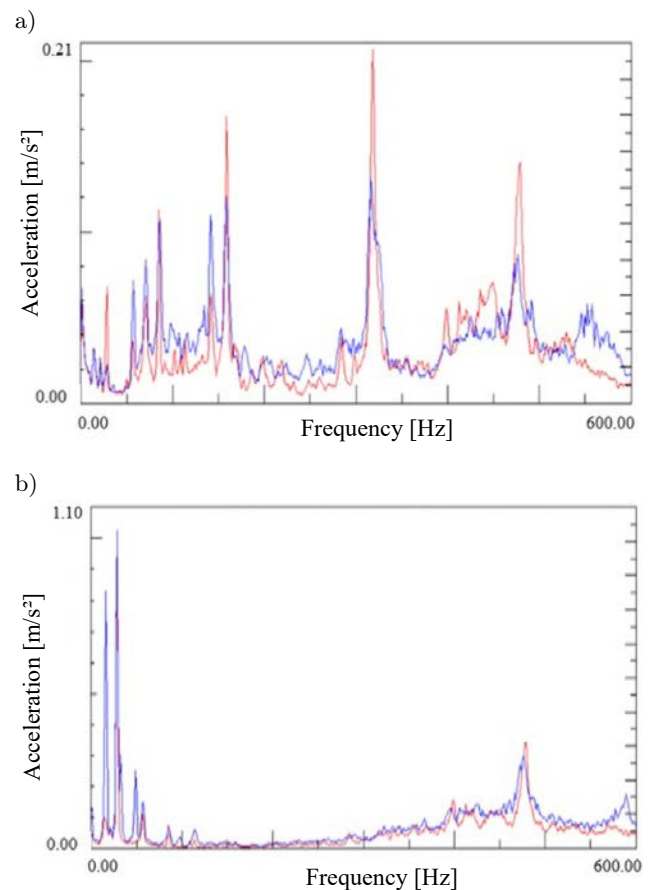
a)

b)

Fig. 8. Acceleration FFT of AC pipe (a) and compressor (b) in the HVAC vehicle, red – AC off, blue – AC on (idle).

b) Operating condition

Since the engine is running at various speeds during the operating condition, a 3D colour map with an order tracking indicator is used to relate the engine speed

with the humming-type noise and vibration induced frequencies and amplitudes (WANG, 2010). Figures 9 and 10 show the results of 3D colour maps for the AC pipe and compressor of the HVAC model system at different AC conditions, respectively. A comparable with the idle condition can be obtained where the AC pipe
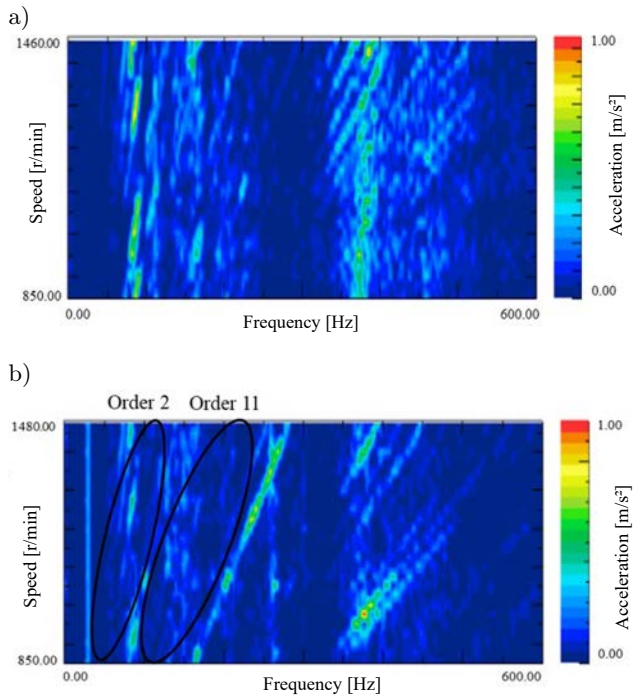
a)

b)

Fig. 9. 3D colour map acceleration of AC pipe when AC is off (a) and AC is on (b) in the HVAC model (operating).
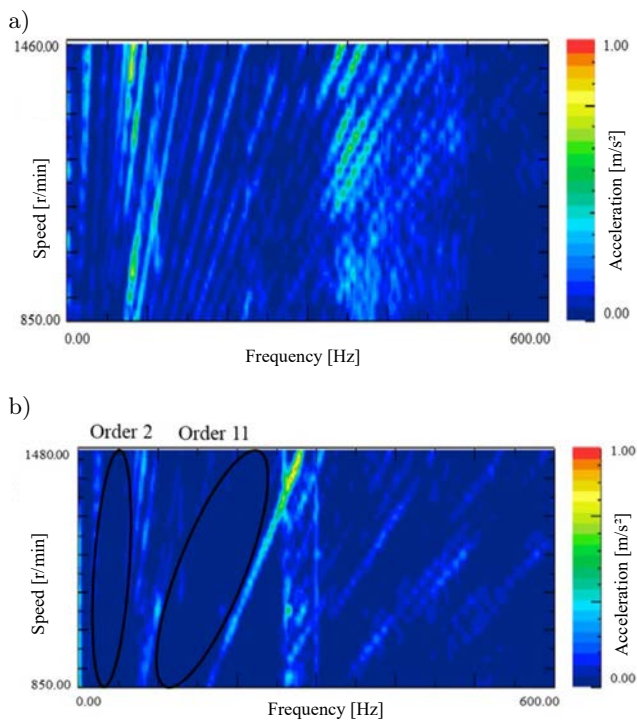
a)

b)

Fig. 10. 3D colour map acceleration of compressor when AC is off (a) and AC is on (b) in the HVAC model (operating).

and compressor have resulted in high acceleration amplitudes between 50–250 Hz (towards reddish contour) of frequency range when the AC is activated. In this range, both components have resulted multiple order levels, which is order 2 and 11 that contributed to the humming-type noise and vibration to the HVAC system as discussed by SATAR et al. (2021b).

The results obtained in the HVAC model is then validated with the vehicle system. Figure 11 shows a 3D colour map of the humming-type noise produced in the vehicle centre cabin at different engine speeds, frequencies, and AC conditions. The figures shows that there are reddish contours which indicates the peak intensity of the humming-type noise between the frequency range of 50–250 Hz when the AC is activated, as determined in the HVAC model. In addition, the order levels obtained are also similar to the HVAC model, which occurred at order 2 and 11. The finding is later been verified using LMS TestLab Sound Diagnosis, and from that, the humming-type noise can be clearly heard at this operating frequency for both idle and operation conditions.
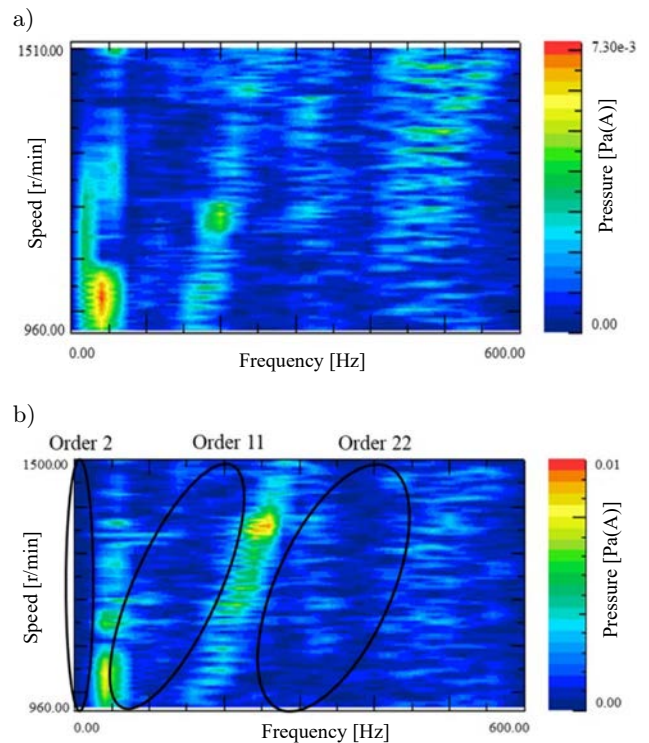
a)

b)

Fig. 11. 3D colour map sound pressure of centre cabin when AC is off (a) and AC is on (b) in the HVAC vehicle (operating).

Table 2 highlights the summary of the humming-type noise and vibration induced in both HVAC model and vehicle systems. From table, it is clear that the root cause of the humming problems is originated from the AC pipe as the main component's contribution due to the resonance of its structure. This humming noise is later propagated to the vehicle cabin as measured

Table 2. Humming noise and vibration result summary for both HVAC model and vehicle systems.

HVAC system	Test conditions	Engine speed [r/min]	Humming frequency range [Hz]	Highest contributed components
Model	Idle	850		AC pipe
	Operating	850–1400	50–250	
Vehicle	Idle	850		AC pipe, centre cabin
	Operating	850–1400		

at the centre AC outlet with a corresponded operating frequency range of 50–250 Hz.

3.3. Effect of the TDVA

3.3.1. TDVA configuration

Based on Eq. (9), the properties required to calculate the length of TDVA for both HVAC model and vehicle systems are shown in Table 3. From the table, the tuned frequency is selected based on the most dominant peaks of the AC pipe FRF without the TDVA attachment, which is 106 Hz for HVAC vehicle and 148 Hz for HVAC models, as shown in Fig. 12. From that, the optimum L values obtained are 0.057 m and 0.051 m for the HVAC model and vehicle systems, respectively.

Table 3. Properties and length of the TDVA for the model and vehicle systems.

Properties	Young modulus E [GPa]	Moment of inertia I [nm^4]	Tuned frequency f [Hz]	Length L [m]
Model system	210	33.2086	148	0.057
Vehicle system			106	0.051

3.3.2. EMA results with TDVA

After the tuning of TDVA, EMA is repeated to observe its effect on the natural frequency values of the AC pipe structure. Figure 12 shows the AC pipe FRF comparison (with and without TDVA) for the HVAC model and vehicle systems, respectively. From the figure of HVAC model, it is found that the most dominant peak of natural frequency at 148 Hz has been eliminated and shifted outside the humming-type noise region when the TDVA is applied to the AC pipe. A new effective frequency range has been determined between 75–255 Hz for the HVAC model with the significant vibration amplitude reduction. Table 4 shows the mode shapes of the highest natural frequency for with and without TDVA. From the table, it can be observed that at 148 Hz (without TDVA), the AC pipe has suffered a bending deflection along the AC pipe structure, and
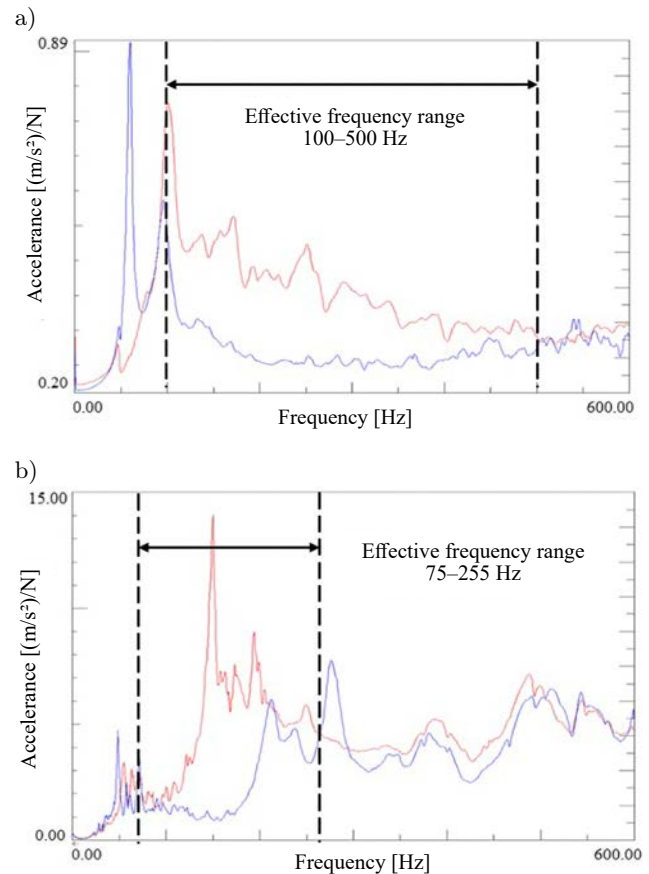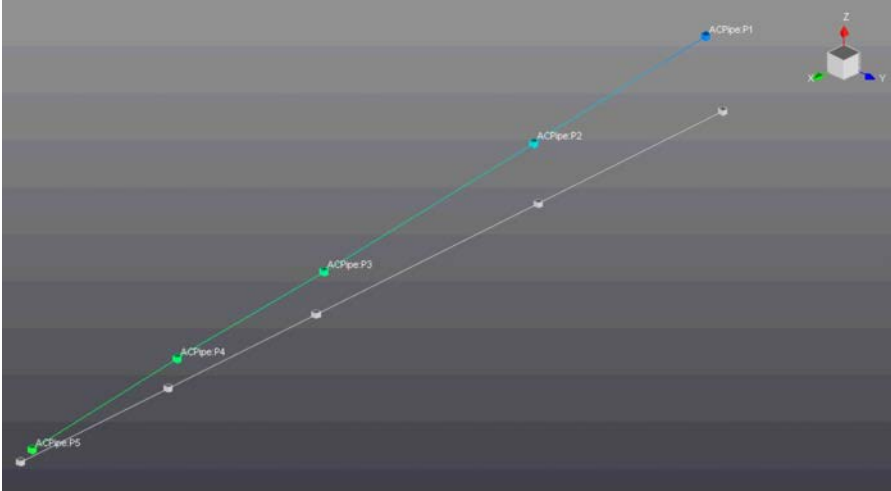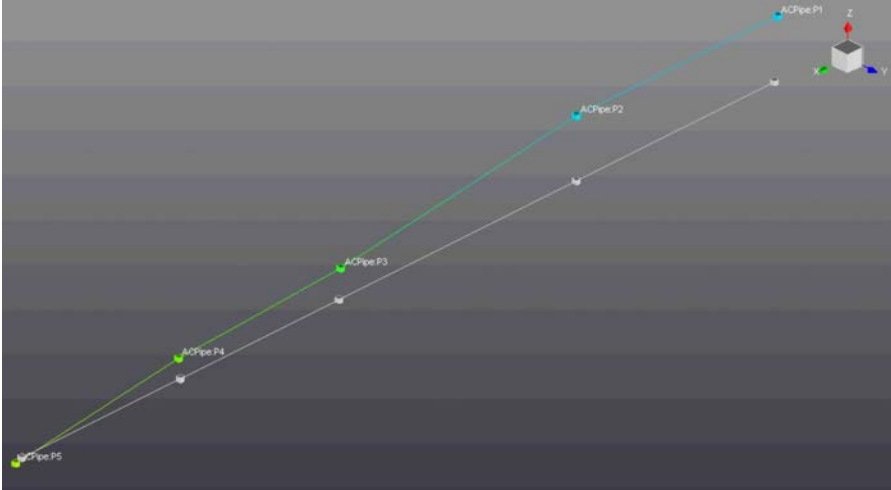

Fig. 12. AC pipe FRF comparison for with (blue) and without (red) the TDVA: a) HVAC vehicle; b) HVAC model.

with the application of TDVA, this motion has been shifted to 275 Hz, which is outside of humming-type noise region.

As for the HVAC vehicle system, the effective frequency range determined become wider, covering of 100–500 Hz of frequencies. This is due to the difference of mounting constraint inside the engine bay. In the HVAC model system, the components are mounted on the rig, while in the vehicle system, the components are mounted on the solid body of the vehicle. The higher mounting stiffness of the vehicle partly contributes to the differences of effective frequency range determined. Significantly, both systems have a good agreement between humming-type region of below 250 Hz and exhibit a similar trend of improvement.

Table 4. Mode shapes of the AC pipe (with and without the TDVA).

Conditions	Highest peak of natural frequency f [Hz]	Mode shapes
Without TDVA	148	
With TDVA	275	

3.3.3. Humming noise and vibration with TDVA

a) Idle condition

Figure 13 shows the acceleration FFT for the AC pipe and compressor in the HVAC model system during an idle condition, respectively. From the figures, the acceleration amplitude of AC pipe (i.e. 0.72 m/s²) and compressor (i.e. 0.69 m/s²) are high in the range of 100–150 Hz for the case of AC is not activated (red colour), which coincides with the natural frequencies of the structures. After the AC is activated, the acceleration of both components is slightly reduced due to the compressor engagement which provides smooth HVAC operation and refrigerant fluids flow as shown in the green line colour. When the TDVA is introduced to the system, the acceleration of the HVAC components

such AC pipe especially, has shown a significant reduction to 0.15 m/s². This result proved that the TDVA is applicable to reduce the vibration of the AC pipe up to 79% in the range of humming-type region.

Similarly, a verification is conducted with the HVAC vehicle system and the result of transmitted noise inside the vehicle cabin centre outlet is presented in Fig. 14. From the figure, when the AC is activated, the noise FFT of the centre cabin shows a slight peak of $1.03 \cdot 10^{-3}$ Pa(A) in the range of humming-type noise. The application TDVA has further reduced the noise in that range significantly as shown in the blue line. As the natural frequency peaks of the AC pipe have been shifted, the originated humming-type noise from the component can also been reduced as shown before in FRF graphs in Fig. 12.
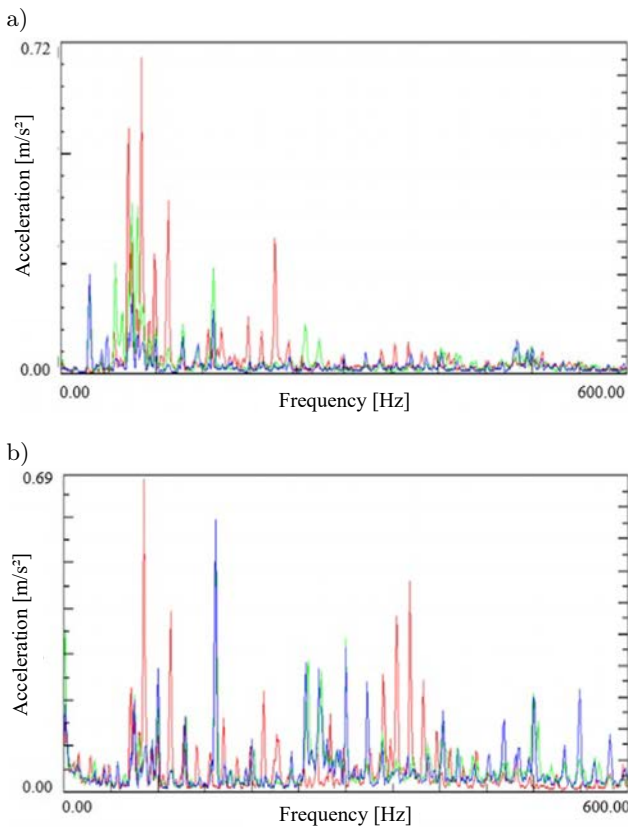
a)

b)

Fig. 13. Acceleration FFT of AC pipe (a) and compressor (b) in the HVAC model; red – AC off, green – AC on without TDVA, and blue – AC on with TDVA (idle).
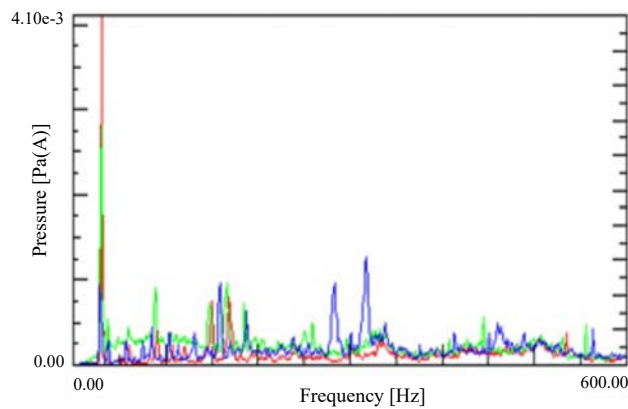

Fig. 14. Sound Pressure FFT of centre cabin in the HVAC vehicle; red – AC off, green – AC on without TDVA, and blue – AC on with TDVA (idle).

b) Operating condition

Figure 15 shows the acceleration FFT for the AC pipe and compressor in the HVAC vehicle system during the operating condition, respectively. From the figures, a significant improvement can be observed for the AC pipe when the TDVA is applied with the activation of AC, whereby the acceleration peak is reduced from 3.1 m/s^2 to 1.2 m/s^2 (i.e. 61%) in the humming frequency range of 50–250 Hz. However, above
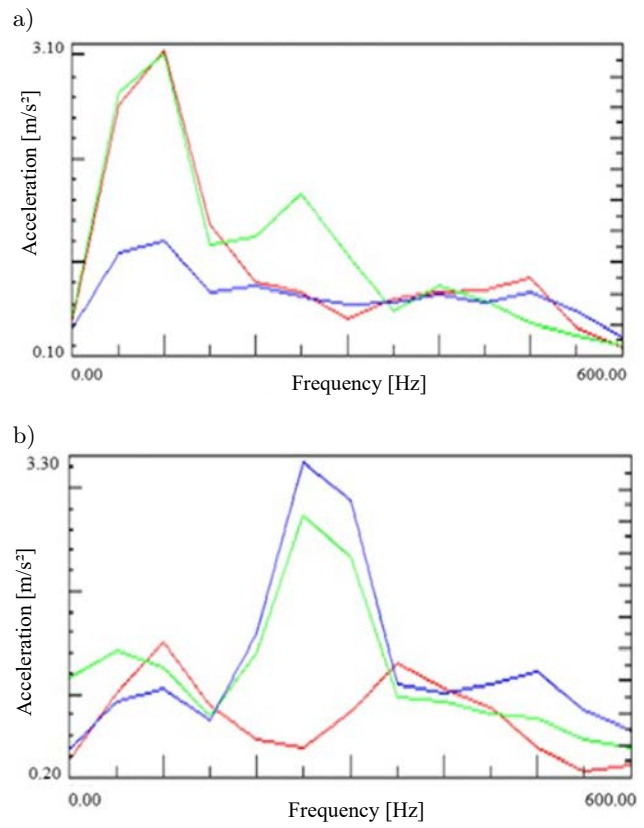
a)

b)

Fig. 15. Acceleration FFT of AC pipe (a) and compressor (b) in the HVAC model; red – AC off, green – AC on without TDVA, and blue – AC on with TDVA (operating).

350 Hz, a consistent trend is observed when comparing of all three AC conditions. Similarly for compressor, the finding showed a significant vibration reduction trend at humming frequency range below 150 Hz. However, it become ineffective after the forementioned since the TDVA is designed and tuned based on the AC pipe structure.

As for the HVAC vehicle system, the validation has been carried out and the acceleration FFT result for the AC pipe is shown in Fig. 16. From the figure, it
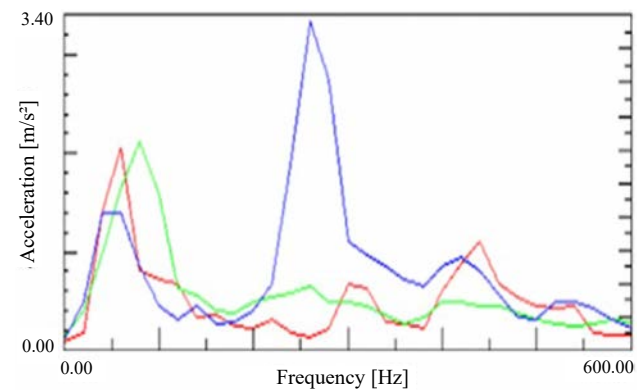

Fig. 16. Acceleration FFT of AC pipe in the HVAC vehicle; red – AC off, green – AC on without TDVA, and blue – AC on with TDVA (operating).

can be observed that the TDVA is effective in reducing the acceleration of the AC pipe in the humming frequency range of 50–200 Hz. However, the TDVA is become ineffective outside the humming-type region of the HVAC vehicle system as the AC pipe has a different structural mounting compared to the HVAC model rig structure. The humming-type noise is later been analysed using LMS TestLab Sound Diagnosis to verify the existing and reduction of the noise.

4. Conclusion

A thorough investigation of the humming-type noise and vibration presence in the vehicle HVAC system and its counter measure using the TDVA have been successfully carried out. Of four suspected HVAC components, the AC pipe is found to be the main source of this problem. From the investigation, the humming-type noise and vibration are occurred in the frequency range of 50–250 Hz for both HVAC idle and operating conditions. The proposed TDVA is able to solve the problem with the effective frequency range of 75–255 Hz and 100–500 Hz, respectively. The study also achieved a good result agreement for the HVAC model and vehicle systems with a total vibration reduction of 79% and 61% for both HVAC idle and operating conditions. This subsequently reduced the induced humming-type noise inside the vehicle cabin.

Acknowledgments

References

1. AHMAD MAZLAN A.Z., MOHD RIPIN Z. (2016), Structural dynamic modification of an active suspended handle with a parallel coupled piezo stack actuator, *Proceedings of the Institution of Mechanical Engineers, Part I: Journal of Systems and Control Engineering*, **230**(2): 130–144. doi: 10.1177/0959651815618840.

2. ALLAM S., ÅBOM M. (2014), Fan noise control using microperforated splitter silencers, *Journal of Vibration and Acoustics*, **136**(3): 031017, doi: 10.1115/1.4027245.

3. ARENAS J.P., CROCKER M.J. (2010), Recent trends in porous sound-absorbing materials, *Sound & Vibration*, **44**(7): 12–18.

4. BRENNAN M.J. (2000), Actuators for active vibration control-tunable resonant devices, *Applied Mechanics and Engineering*, **5**(1): 63–74.

5. EILEMANN A. (1999), Practical noise and vibration optimization of HVAC systems, *SAE International*, doi: 10.4271/1999-01-0867.

6. ESMAILZADEH E., JALILI N. (1998), Optimum design of vibration absorbers for structurally damped Timoshenko beams, *Journal of Vibration and Acoustics*, **120**(4): 833–841, doi: 10.1115/1.2893908.

7. FATIMA S., MOHANTY A.R. (2011), Acoustical and fire-retardant properties of jute composite materials, *Applied Acoustics*, **72**(2–3): 108–114, doi: 10.1016/j.apacoust.2010.10.005.

8. FORMENT D., WELARATNA S. (1981), Structural dynamics modification – an extension to modal analysis, *SAE International*, doi: 10.4271/811043.

9. GREN E., FARRALL M., MENDONÇA F., SANDHU K. (2012), CFD prediction of aeroacoustic noise generation in a HVAC duct, [in:] *In 18th AIAA/CEAS Aeroacoustics Conference (33rd AIAA Aeroacoustics Conference)*, doi: 10.2514/6.2012-2068.

10. HAO K.Y., MEI L.X., RIPIN Z.M. (2011), Tuned vibration absorber for suppression of hand-arm vibration in electric grass trimmer, *International Journal of Industrial Ergonomics*, **41**(5): 494–508, doi: 10.1016/j.ergon.2011.05.005.

11. HASHI H.A., MUTHALIF A.G.A., DIYANA NORDIN N.H. (2016), Dynamic tuning of torsional transmissibility using magnetorheological elastomer: modelling and experimental verification, *Iranian Journal of Science and Technology, Transactions of Mechanical Engineering*, **40**: 181–187, doi: 10.1007/s40997-016-0024-6.

12. HE J., FU Z.-F. (2001), Mathematics for modal analysis, *Modal Analysis*, **2001**: 12–48, doi: 10.1016/b978-075065079-3/50002-4.

13. IMAHIGASHI S., SAKAI M., YOSHINO E., MITSUISHI Y. (2016), Compact high-efficiency 2-layer blower fan for HVAC, *SAE International*, doi: 10.4271/2016-01-0193.

14. KURNIAWAN D., ROGERS E. (2011), Investigation of airflow induced whistle noise by HVAC control doors utilizing a "V-shape" rubber seal, *SAE International*, doi: 10.4271/2011-01-1615.

15. MAVURI S.P., WATKINS S., WANG X., ST. HILL S., WEYMOUTH D. (2008), An investigation of vehicle HVAC cabin noise, *SAE International*, doi: 10.4271/2008-01-0836.

16. PARIKH D.V., CHEN Y., SUN L. (2006), Reducing automotive interior noise with natural fiber nonwoven floor covering systems, *Textile Research Journal*, **76**(11): 813–820, doi: 10.1177/0040517506063393.

17. SAIFUDIN M.I.A.-M., USAMAH N.M., RIPIN Z.M. (2018), Attenuation of motorcycle handle vibration using dynamic vibration absorber, *MATEC Web of Conferences*, **217**: 01006, doi: 10.1051/matecconf/201821701006.

18. SATAR M.H.A. *et al.* (2019), Application of the structural dynamic modification method to reduce the

vibration of the vehicle HVAC system, *Journal of Physics: Conference Series*, **1262**(1): 012034, doi: 10.1088/1742-6596/1262/1/012034.

19. SATAR M.H.A., MAZLAN A.Z.A., HAMDAN M.H., ISA M.S.M., PAIMAN M.A.R., GHAPAR M.Z.A. (2021a), A lab-scale HVAC hissing-type noise characterization with vehicle system validation, *Archives of Acoustics*, **46**(2): 365–373, doi: 10.24425/aoa.2021.136589.

20. SATAR M.H.A., MAZLAN A.Z.A., HAMDAN M.H., ISA M.S.M., PAIMAN M.A.R., GHAPAR M.Z.A. (2021b), Experimental validation of the HVAC humming-type noise and vibration in model and vehicle system levels, *Archives of Acoustics*, **46**(2): 375–385, doi: 10.24425/aoa.2021.136590.

21. SIMION M., SOCACIU L., UNGURESAN P. (2016), Factors which influence the thermal comfort inside of vehicles, *Energy Procedia*, **85**: 472–480, doi: 10.1016/j.egypro.2015.12.229.

22. SINGH S., MOHANTY A.R. (2018), HVAC noise control using natural materials to improve vehicle interior sound quality, *Applied Acoustics*, **140**: 100–109, doi: 10.1016/j.apacoust.2018.05.013.

23. SINGH S., PAYNE S.R., JENNINGS P.A. (2014), Toward a methodology for assessing electric vehicle exte- rior sounds, *IEEE Transactions on Intelligent Transportation Systems*, **15**(4): 1790–1800, doi: 10.1109/tits.2014.2327062.

24. THAWANI P.T., SINADINOS S., BLACK J. (2013), Automotive AC system induced refrigerant hiss and gurgle, *SAE International Journal of Passenger Cars – Mechanical Systems*, **6**(2): 1115–1119, doi: 10.4271/2013-01-1890.

25. WALLACK P., SKOOG P., RICHARDSON M. (1989), Comparison of analytical and experimental rib stiffener modifications to a structure, [in:] *International Modal Analysis Conference*, **2**: 965–973.

26. WANG S., GU J., DICKSON T., DEXTER J., MCGREGOR I. (2005), Vapor quality and performance of an automotive air conditioning system, *Experimental Thermal and Fluid Science*, **30**(1): 59–66, doi: 10.1016/j.expthermflusci.2005.03.019.

27. WANG X. [Ed.] (2010), *Vehicle noise and vibration refinement*, Elsevier, doi: 10.1016/b978-1-84569-497-5.50018-2.

28. XI J., FENG Z., WANG G., WANG F. (2015), Vibration and noise source identification methods for a diesel engine, *Journal of Mechanical Science and Technology*, **29**(1): 181–189, doi: 10.1007/s12206-014-1225-9.